

Computational and Experimental Investigations of the Formal Dyotropic Rearrangements of Himbert Arene/Allene Cycloadducts

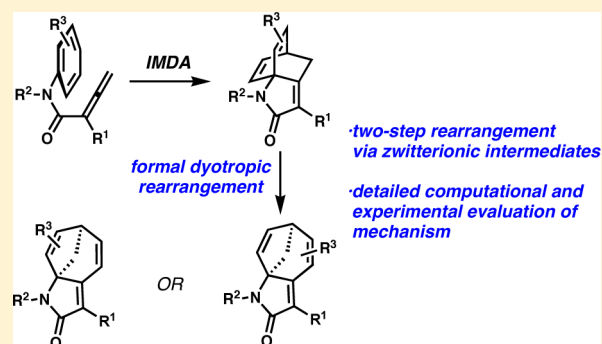
Hung V. Pham,^{†,§} Alexander S. Karns,^{‡,§} Christopher D. Vanderwal,^{*,‡} and K. N. Houk^{*,†}

[†]Department of Chemistry and Biochemistry, University of California, Los Angeles, 607 Charles E. Young Drive, Los Angeles, California 90095-1569, United States

[‡]1102 Natural Sciences II, Department of Chemistry, University of California, Irvine, California 92697-2025, United States

S Supporting Information

ABSTRACT: The fascinating intramolecular arene/allene cycloaddition discovered by Himbert affords dearomatized, polycyclic intermediates with sufficient strain energy to drive rearrangement processes of the newly formed ring system. We disclose a detailed examination of a thermally induced stepwise dyotropic skeletal rearrangement of these cycloadducts, a reaction also first described by Himbert. We offer computational evidence for a two-stage mechanism for this formal dyotropic rearrangement and provide rationalizations for the significant substitution-dependent rate differences observed in experiments. These investigations led to the development of a Lewis-acid-catalyzed rearrangement of precursors that were unreactive under simple thermal instigation. The isolation of the product of an “interrupted” rearrangement under Lewis acidic conditions provides further support for the proposed stepwise mechanism. Computational results also matched experiments in terms of regiochemical preferences in unsymmetrical rearrangement precursors and explained why lactam O-, S-, and C-heterologues do not easily undergo this rearrangement.



INTRODUCTION

Over the past several years, our research groups have been collaboratively investigating the mechanistic details¹ and synthetic utility² of a fascinating dearomatizing cycloaddition³ originally discovered by Himbert and Henn.^{3a} The subject reactions convert allenecarboxanilides and closely related arene/allenes into bridged, topologically complex, and relatively strained tricyclic cycloadducts (**1** → **2**, Figure 1) with great potential for thermodynamically driven rearrangement to other

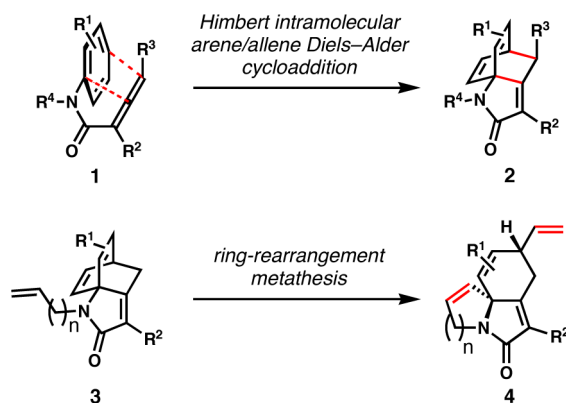


Figure 1. Himbert arene/allene cycloaddition and the ring-rearrangement metathesis (RRM) of select alkene-bearing cycloadducts.

ring systems. For example, we have studied in some detail the ring-rearrangement metathesis of Himbert cycloadducts bearing tethered alkenes (**3** → **4**).^{2,4} In this disclosure, we share the results of our computational and experimental investigations of a formal dyotropic shift that converts Himbert cycloadducts into rearranged tricyclic products.^{3c,5}

BACKGROUND

Dyotropic Rearrangements. Dyotropic rearrangements are a special type of pericyclic process defined by Reetz in the 1970s^{6,7} that have been leveraged in complex molecule synthesis⁸ and subjected to a range of mechanistic investigations.^{9,10} Reetz distinguished Type I rearrangements,^{6a} where two σ bonds interchange positions, from Type II rearrangements, where two σ bonds both move to new bonding sites with a repositioning of a π -bond.^{6b} Mechanistic investigations have shown that the Type I dyotropic shift can occur through either concerted or stepwise pathways (Figure 2).¹⁰ The stepwise reaction can be described as sequential pinacol-like shifts that cause interconversion of the positions of two groups in a vicinal arrangement.

Himbert Cycloadditions and the Formal Dyotropic Rearrangement. In certain cases, Himbert observed interesting Type I dyotropic shift products upon heating some of these

Received: April 15, 2015

Published: May 11, 2015

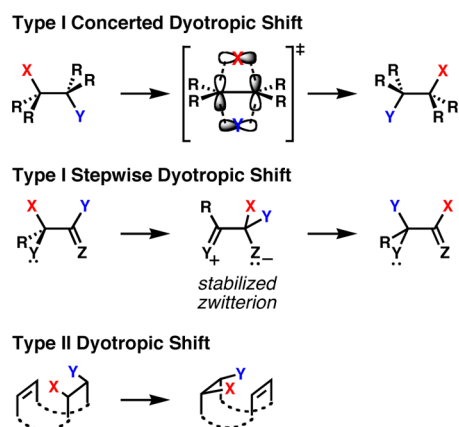
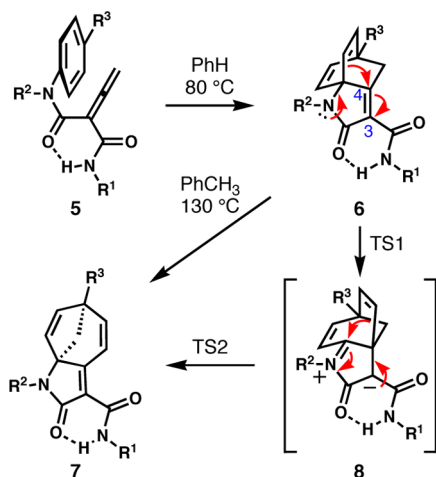


Figure 2. Type I and Type II dyotropic rearrangements.

cycloadducts.^{3c,5} In particular, those substituted with an amide functionality α to the carbonyl of the lactam—cycloadducts that were formed under relatively mild conditions—*isomerized* efficiently from the bicyclo[2.2.2]octadiene **6** to the bicyclo[3.2.1]octadiene product **7** (Scheme 1). By changing the

Scheme 1. Formal Dyotropic Rearrangement of Himbert Cycloadducts



substituents at various positions and measuring the kinetics of the rearrangement (see Table 1), Himbert proposed a stepwise mechanism involving zwitterionic intermediate **8**;¹¹ he reasoned that the experimentally measured half-lives of a number of substrates correlated with the charge-stabilizing ability of the substituents. Trifonov and Orahovats, who also

Table 1. Substituent Effects on Rearrangement Rates^a

entry	R ¹	R ²	R ³	<i>t</i> _{1/2} (h)
1	<i>i</i> -Pr	Me	H	21
2	<i>c</i> -Hex	Me	H	23
3	Ph	Me	H	7
4	1-Naph	Me	H	—
5	<i>t</i> -Bu	Ph	H	230
6	Ph	Ph	H	52
7	Ph	Me	Me	5
8	Ph	Me	Br	1

^aData from ref 11.

studied the thermal arene/allene cycloaddition,¹² uncovered a photochemical rearrangement closely related to that shown in Scheme 1; however, success in that reaction was confined to a narrow range of substrates.¹³

From our perspective, and consistent with Himbert's proposal, a concerted mechanism is unlikely in these systems, owing to the C3–C4 alkene disallowing *anti* alignment of the migrating orbitals typically seen in single-step dyotropic rearrangements. We report a computational investigation of the formal dyotropic rearrangement observed in Himbert cycloadducts, including an elucidation of substituent effects on the rates of these reactions and experimental validation of some of our predictions.

RESULTS AND DISCUSSION

Computational Methods. All stationary point structures were optimized using the B3LYP functional,¹⁴ with a 6-31G(d) basis set in Gaussian09.¹⁵ Single-point calculations were conducted with M06-2X/6-311+G(d,p) on the B3LYP optimized geometries. In general, B3LYP and M06-2X produce similar optimized geometries.¹⁶ For iodine-containing compounds, split basis sets were necessary: optimizations used the LANL2DZ basis set¹⁷ for iodine and 6-31G(d) for the remaining atoms, while single points used the SDD basis set¹⁸ for iodine and 6-311+G(d,p) for the remaining atoms. Vibrational frequencies were computed to determine the nature of each stationary point; local minima and transition structures showed 0 and 1 imaginary frequency, respectively. Partial atomic charges were calculated using a natural bond orbital (NBO) analysis.¹⁹ The Conductorlike Polarizable Continuum Model (CPCM) simulated implicit xylene solvent for optimizations and single-point calculations.²⁰ All energies were computed for reactions at 298 K.

Mechanism of the Parent Reaction. We first explored the parent system **9a** (Figure 3), formed via the intramolecular

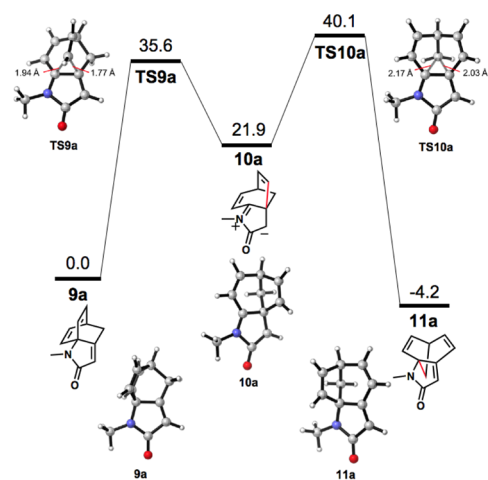


Figure 3. Reaction coordinate diagram of the formal dyotropic rearrangement of **9a**. Optimized structures and relevant bond-forming and bond-breaking distances are shown. Energies are in kcal/mol.

[4 + 2] cycloaddition of *N*-phenyl-*N*-methyl allenecarboxamide. Rearrangement of **9a** delivers product **11a**. DFT-optimized structures of substrate **9a** and subsequent rearrangement stationary points are reproduced in this figure. The rearrangement occurs via a stepwise mechanism, passing through a stabilized zwitterionic intermediate **10a**. Although concerted

dyotropic shifts for other systems are known,^{10c,f,g,i,j,l,m,n} a concerted transition state could not be located, presumably because of the difficulty of achieving appropriate overlap in a transition state involving this tricyclic system. The lone pair on the nitrogen of the lactam promotes the initial migration of one of the vinyl groups through **TS9a**, which exhibits short bond-forming and bond-breaking lengths of 1.77 and 1.94 Å. Although vinyl shifts are not commonly seen, the migratory aptitude of the vinyl group is much larger than that for a methylene group, which explains the lower activation energy for **TS9a**.²¹ In their kinetic studies of vinyl migrations using the phenanthrenium cation, Bushmelev and co-workers determined that the migration occurs in a 1,2-sigmatropic fashion rather than through mechanisms involving discrete cationic intermediates with completely severed bonds.²² Similarly, we did not observe these types of intermediates in the Himbert system. However, it is conceivable that the π -orbital of the migrating vinyl group could be interacting favorably with the π -orbital of the enone, which ultimately forms the new σ -bond in **10a**. We generated and compared the HOMO orbitals of **9a** and **TS9a** using a natural bonding orbital (NBO) analysis; examination of the relevant π -orbitals and inspection of the vinyl dihedral angle along the reaction path validate the significance of these orbital interactions in stabilizing the sigmatropic shift (see Supporting Information).

Zwitterionic intermediate **10a** is 21.9 kcal/mol less stable than **9a**, despite the stabilization of the cation by the neighboring nitrogen atom and the delocalization of the anion through conjugation with the carbonyl. Moderate charge transfer (defined as the difference in charge per atom relative to starting substrate **9a**) indicates the zwitterionic nature of the intermediate; an unrestricted DFT calculation yields an S^2 value of 0, indicating a closed-shell species. Furthermore, changing the intrinsic solvent from xylenes to the more polar aqueous environment stabilized the intermediate and transition states by 2 kcal/mol, indicative of polarized species, without changing the product energy.

The subsequent methylene migration **TS10a** alleviates the charge separation and is the rate-determining step of the rearrangement, requiring 18.2 kcal/mol from intermediate **10a** (40.1 kcal/mol from **9a**) to form thermodynamically favored product **11a**; this large barrier is corroborated by the low yield of **11a** observed experimentally (see below), despite the extended conjugation and reduced strain leading to an exergonic reaction. The forming and breaking bond lengths of 2.17 and 2.03 Å are longer than those in **TS9a**, an unsurprising result since the methylene sp^3 orbital holds electrons less tightly than the vinyl sp^2 orbital, owing to the increased s character of the latter. The absence of π -orbital interaction that is observed in **TS9a** explains the higher activation energy of **TS10a**. Stabilization of this transition state would decrease the kinetic barrier and result in a more facile rearrangement.

To determine whether ring strain is important in the transformation of the bicyclo[2.2.2]octadiene to the bicyclo[3.2.1]octadiene moiety, optimizations of the two parent bicyclic molecules were conducted (Figure 4). The bicyclo[3.2.1]octadiene is minimally more stable than its bicyclo[2.2.2]octadiene precursor, with only a 0.3 kcal/mol energy difference. Addition of an *exo*-methylidene group to better simulate the Himbert cycloadduct substrate increases the difference to 3.4 kcal/mol in favor of the bicyclo[3.2.1]octadiene isomer, likely owing to the incorporation of another

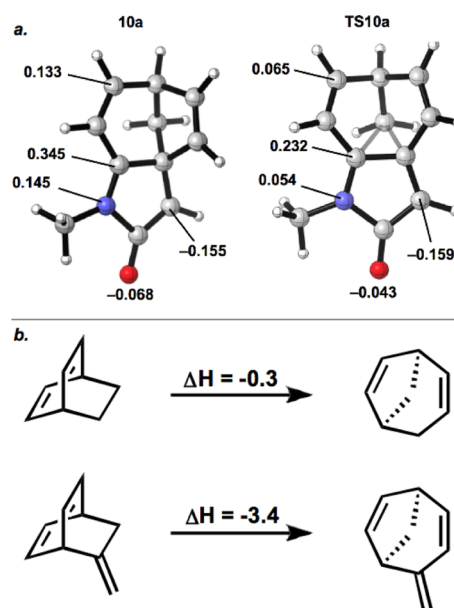
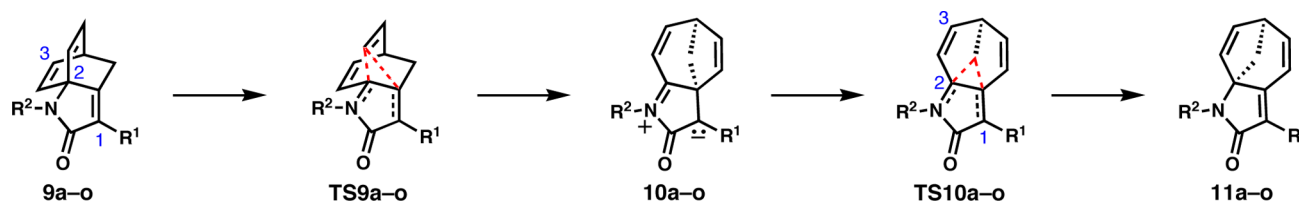


Figure 4. (a) Charge transfer in the zwitterionic intermediate **10a** and transition structure **TS10a**, relative to **9a**. (b) Contribution of ring strain to reaction energetics.

sp^2 -hybridized carbon atom into the bicyclic system along with the added conjugation of the diene. This alleviation of ring strain is also manifested in the exothermicity of the overall rearrangement reaction shown in Figure 4b and also for the conversion of **9a** into **11a**.

Electronic Activation of the Rearrangement. Owing to the charge separation that develops after the 1,2-vinyl shift, substituents at the α -position of the lactam should have a large effect on the stability of intermediates of type **10a**, and subsequently the rate-determining transition state **TS10a**. Himbert observed that the dyotropic rearrangement occurred only in compounds with an amide functionality α to the carbonyl of the lactam (Scheme 1);^{3c,5} presumably the anion-stabilizing ability of the electron-withdrawing amide promotes the migration. However, it was unclear to what extent the hydrogen bonding arrangements shown in structures **6–8** were important to the feasibility of the rearrangements. This question prompted us to probe the effects of various substituents at the α position of the lactam carbonyl.

In Table 2, we provide the free energies of the stationary points for the parent unsubstituted cycloadduct (**9a**) as well as the α -substituted analogs (**9b–9k**). The relative rate constants calculated from the Eyring equation using the activation energies of **TS10** are also provided. The exergonicity of the reaction remains relatively consistent across the range of substrates at 2–6 kcal/mol. Substitution with an α -methyl group slightly increases the energies of the intermediate and transition states. When an amide substituent is incorporated (entries c–e), the free energies of the rate-determining **TS10** drop substantially by 6 kcal/mol, consistent with the ability of these substrates to undergo the rearrangement experimentally. The transition state free energies of the phenylamide-substituted substrate (**9d**) are stabilized by 1 kcal/mol relative to the methylamide substrate (**9c**) owing to the better delocalization of the negative charge. The dimethylamido substituent (**9e**) is less electron-withdrawing than its primary amide counterparts, resulting in a higher barrier for rearrangement, although hydrogen bonding could also be at play.

Table 2. Calculated Free Energies, Partial Atomic Charges, and Theoretically Derived Relative Rates for Stepwise Dyotropic Rearrangements of a Range of Himbert Cycloadducts^a

Entry	R ¹	R ²	Free Energies				Relative Partial Charge Transfer (TS10)					k _{rel}
			TS9	10	TS10	11	O	C1	N	C2	C3	
a	H	Me	35.6	21.9	40.1	-4.2	0.000	0.000	0.000	0.000	0.000	1
b	Me	Me	36.2	23.7	41.6	-5.9	-0.007	0.019	0.002	-0.003	-0.003	1.5 × 10 ⁻¹
c	CONHMe	Me	31.0	15.6	34.8	-3.3	0.018	0.043	-0.018	0.004	0.000	7.5 × 10 ²
d	CONHPh	Me	30.0	14.4	33.8	-3.2	0.048	0.184	-0.003	0.005	0.000	12.6 × 10 ³
e	CONMe ₂	Me	31.4	15.2	36.1	-3.8	0.015	0.030	-0.013	-0.002	0.000	1.5 × 10 ²
f	CH ₂ OH	Me	35.8	23.6	40.7	-4.3	-0.003	0.026	-0.006	-0.002	-0.003	4.7 × 10 ⁻¹
g	F	Me	39.2	26.5	44.3	-4.5	-0.012	0.024	0.000	-0.012	-0.003	5.3 × 10 ⁻³
h	CHO	Me	27.5	9.7	30.7	-3.3	0.035	0.058	-0.021	0.004	0.001	1.2 × 10 ⁵
i	NO ₂	Me	26.5	7.6	29.7	-2.7	0.042	0.071	-0.022	-0.002	0.001	4.3 × 10 ⁵
j	CN	Me	29.1	12.5	32.6	-4.1	0.023	0.033	-0.015	0.001	0.001	1.2 × 10 ⁴
k	SiMe ₃	Me	34.3	19.9	39.0	-3.6	0.008	-0.008	-0.004	0.005	0.001	3.9
l	H (+BF ₃)	Me	29.8	15.6	34.2	-4.2	0.000	0.080	-0.045	-0.011	-0.006	1.6 × 10 ³
m	CONHMe	Ph	31.1	18.7	36.2	-1.5	0.012	-0.021	-0.039	0.012	-0.007	1.3 × 10 ²
n	CONHMe	<i>p</i> -OMePh	30.3	17.3	35.2	-2.4	0.017	-0.022	-0.010	0.012	-0.008	4.5 × 10 ²
o	CONHMe	SiH ₃	32.2	19.5	36.0	-3.2	-0.001	0.048	-0.004	0.015	0.001	1.7 × 10 ²

^aHighlighted entries are for $k_{rel} < 1$ (red), $k_{rel} \cong 1$ (yellow), $k_{rel} \gg 1$ (green).

Saalfrank and co-workers observed that a related *N*-methyl-*N*-phenyl amide substrate (not shown, with other substituents on the allene) spontaneously underwent the dyotropic rearrangement under the conditions used to effect cycloaddition; the initial cycloadduct could not be isolated.²³ However, the tertiary amide group and allene substitution likely conspire to depress the rate of the IMDA reaction, requiring 150 °C to effect cycloaddition (compared to the 130 °C in prior cases). At this temperature, the dyotropic rearrangement occurs spontaneously and only isomerized bicyclo[3.2.1]octadiene was isolated. The hydroxymethyl-substituted system (9f) has a 40.7 kcal/mol activation barrier, intermediate between the unsubstituted and methyl-substituted substrates; the presence of a potential hydrogen bond donor does not appreciably lower the activation barrier TS10. However, replacement with a fluorine atom greatly increases TS10 to 44.3 kcal/mol (entry g). The large electronegativity of fluorine is overshadowed by its π -donation, causing unfavorable electrostatic repulsion. Electron-withdrawing groups at the α -position lower the activation energies in accord with their known anion stabilization abilities (NO₂ > CHO > CN, entries h–j). The zwitterionic intermediates that benefit most from the anionotropy of the α -substituents lie only 7.6–12.5 kcal/mol higher than the starting Himbert cycloadducts, approximately 10 kcal/mol lower than in the unsubstituted case. The trimethylsilyl group shows virtually no change in transition state energy (see entry k); the low-lying vacant orbitals on silicon have only a marginal anion-stabilizing effect.

To corroborate the notion that charge delocalization is stabilizing the rate-determining transition state, we computed NBO charges to discern the amount of charge transfer from 9 to TS10. We focused on the most relevant atoms, i.e. those that

possess a substantial formal charge in the resonance hybrid of 10, namely the oxygen and nitrogen atoms of the lactam and the carbon atoms labeled C1, C2, and C3 (Table 2). The partial charge transfers are reported relative to the parent unsubstituted case, in which all atoms have been set to 0. The calculated rate constants correlate well with the relative amount of charge developed on the carbonyl oxygen, consistent with our earlier predictions. Substituents that withdraw electron density away from the carbonyl in the transition state, through either resonance or induction, will lower the activation energy and increase the rate of reaction. A graph of $\log(k_{rel})$ vs the extent of charge transfer on oxygen (Figure 5) shows a definite linear trend, albeit with an R^2 value of only 0.73; the presence

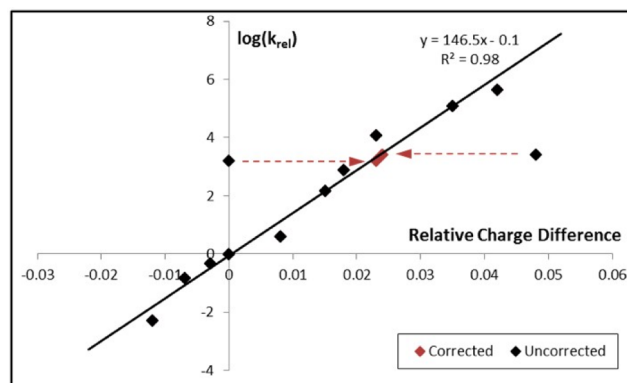
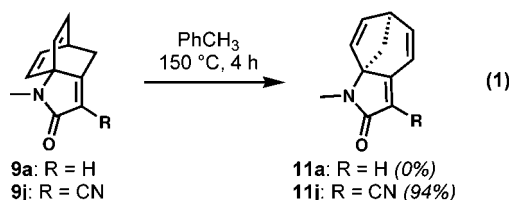


Figure 5. Graph of the correlation between the calculated reaction rate, $\log(k_{rel})$, and the charge difference on the carbonyl oxygen when going from 9b–o to TS10b–o, relative to the parent unsubstituted 9a. Please refer to the text for a discussion of the outlying data points.

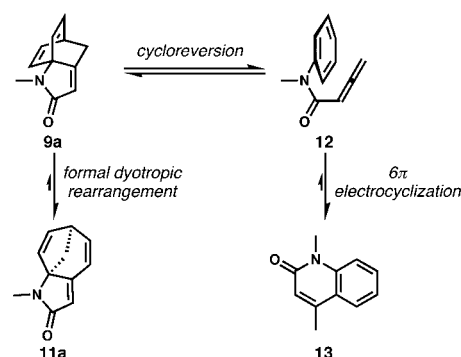
of two outliers—the α -phenylamido and the Lewis acid-catalyzed reactions—diminishes the correlation. For the α -phenylamido substituent, a large portion of the negative charge resides on the oxygen of the amide substituent rather than the lactam. Similarly, the coordinated BF_3 molecule inherits the majority of the negative charge. Thus, inclusion of these other atoms in the charge difference calculation should provide a more accurate representation. When these two factors are corrected for, the coefficient of determination increases to 0.98, implying a strong correlation between the electron-withdrawing ability of the α -substituent and the predicted reaction rate.

To validate our predictions, we turned to experiment. As suggested by calculations, the introduction of a nitrile substituent in the α -position of the α,β -unsaturated lactam will significantly lower the temperature required for the dyotropic shift (see entry j, Table 2). Indeed, we found that heating nitrile-substituted cycloadduct **9j** at 150 °C in toluene produced rearranged product **11j** in 94% yield (eq 1). When parent cycloadduct **9a** was subjected to identical conditions, we observed no reactivity.



Rate Acceleration by Lewis Acids. With delocalization of the anionic charge contributing most toward decreasing the activation barrier of the rearrangement, we postulated that Lewis acid complexation to the lactam carbonyl could facilitate a formal dyotropic shift in substrates that do not rearrange under purely thermal conditions at readily accessible temperatures.²⁴ As expected, calculations on the parent substrate **9a** in the presence of boron trifluoride (entry l, Table 2) showed that the free energies for both transition states and the zwitterionic intermediate are each lowered by about 6 kcal/mol, comparable to the successful α -amido-substituted substrates with which Himbert uncovered this reactivity. Therefore, Lewis acid activation should permit these rearrangements to proceed without the presence of a second activation group. That advance would be significant because the synthesis of the doubly activated allene precursors to the Himbert cycloaddition are troublesome, owing to issues of stability.

Our experimental results were consistent with the computational predictions. Attempts to effect rearrangement of the parent compound **9a** without Lewis acid activation resulted in poor yields, even at 250 °C (Figure 6). At these temperatures, we observed predominant formation of quinolone **13**, presumably resulting from cycloreversion and subsequent electrocyclization. Screening of a variety of Lewis acid catalysts (not shown) led to the discovery that TMSOTf, in combination with 2,4-di-*tert*-butylpyridine to scavenge any liberated triflic acid, was optimal. Without the pyridine base and at 200 °C, the formal dyotropic shift product **11a** was produced in 74% yield, accompanied by unidentifiable decomposition products, which were suppressed by inclusion of the base. Furthermore, an excellent yield of **11a** could be obtained at temperatures as low as 100 °C using conventional heating. We note that the use of boron trifluoride (the Lewis acid used in the computations shown in Table 2), with or without acid scavengers, led to appreciable decomposition.



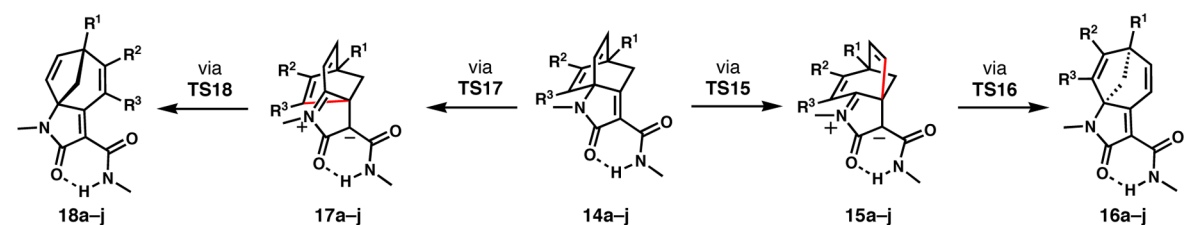
Conditions	11a
<i>o</i> -DCB, 250 °C, μ wave	12% ^a
TMSOTf(0.5), <i>o</i> -DCB, 200 °C, μ wave	74%
TMSOTf(0.5), DTBP ^b (0.1), <i>o</i> -DCB, 200 °C, μ wave	99%
TMSOTf(0.5), DTBP(0.1), PhMe, 100 °C	92%

Figure 6. Lewis acid catalysis of the formal dyotropic rearrangement of Himbert cycloadduct **9a**. ^aThe major product was quinolone **13**. ^bDTBP: 2,4-di-*tert*-butylpyridine.

Effects of Lactam Nitrogen Substituents. The electronic nature of the *N*-substituent of the lactam should influence the stability of the iminium ion portion of the zwitterionic intermediate and should, therefore, impact the energetics of the methylene shift transition state. Table 2 shows that replacing the methyl group of **9c** with a phenyl group (**9m**) raises the energy of **TS10**, likely owing to the electron-withdrawing nature as well as conjugative properties of the substituent. The more electron-donating *p*-methoxyphenyl substituent mitigates the presumed iminium destabilization (compare **9m** and **9n**). Not surprisingly, a silyl group (**9o**) offers no further stabilization of the neighboring positive charge. *N*-Substitution effects are small, leading to computed changes of ca. 2 kcal/mol; the lesser impact of nitrogen substitution relative to α -carbon substitution is likely due to the effects being purely inductive, compared to the electron delocalization offered by the more influential α -substituents.

Effects of the Bicyclo[2.2.2]octadiene Substituents. Given that the dyotropic rearrangement converts the bicyclo[2.2.2]octadiene system to its bicyclo[3.2.1]octadiene isomer, substitution directly on the bridged bicycle should influence the energetics of the reaction. Himbert observed that methyl substitution at the bridgehead carbon (R^1) led to virtually unchanged reaction rates, while bromide at that position resulted in a 7-fold rate increase.⁵ Various positions on the bicyclo[2.2.2]octadiene were considered (Table 3). Entries a–f show the computed free energies for substrates with different R^1 substituents. Relative to the parent reaction, substitution with a methyl, fluoro, or silyl group does not significantly alter the energy of the rate-determining **TS16** (equivalent to **TS10a** in Figure 3) migration. However, the incorporation of bromine lowers the activation barrier by 1.4 to 33.4 kcal/mol, consistent with experimental observation. Switching to an iodine further decreases the barrier to 32.4 kcal/mol, providing evidence that the stabilization is due to more than a simple inductive or steric argument. Examination of the structures of **TS15** reveals increased C–X bond lengths and shorter C–C bonds for the bromo- and iodo-substituted compounds (Figure 7), indicative of previously studied negative hyperconjugative effects (see **22'**).²⁵ Donation of electron density from the migrating carbon

Table 3. Reaction Free Energies of the Formal Dyotropic Rearrangements of Himbert Cycloadducts Substituted on the Bicyclo[2.2.2]octadiene^a



Entry	R ¹	R ²	R ³	TS15	15	TS16	16	TS17	17	TS18	18
a	H	H	H	31.0	15.6	34.8	-3.3	—	—	—	—
b	Me	H	H	31.2	15.7	34.9	-3.9	—	—	—	—
c	F	H	H	31.7	14.8	34.3	-5.0	—	—	—	—
d	Br	H	H	31.8	15.1	33.4	-4.4	—	—	—	—
e	I	H	H	31.0	14.6	32.4	-4.9	—	—	—	—
f	SiH ₃	H	H	31.9	16.5	35.0	-3.0	—	—	—	—
g	H	OMe	H	29.9	8.9	31.9	-4.8	28.7	14.9	33.3	-7.7
h	H	H	OMe	34.6	20.1	38.4	-2.6	32.9	15.8	33.4	6.0
i	H	NO ₂	H	31.8	19.2	36.7	-2.6	34.0	16.0	35.4	-3.4
j	H	H	NO ₂	37.6	23.5	39.6	-1.7	38.3	17.3	34.8	4.3

^aAll energies in kcal/mol.

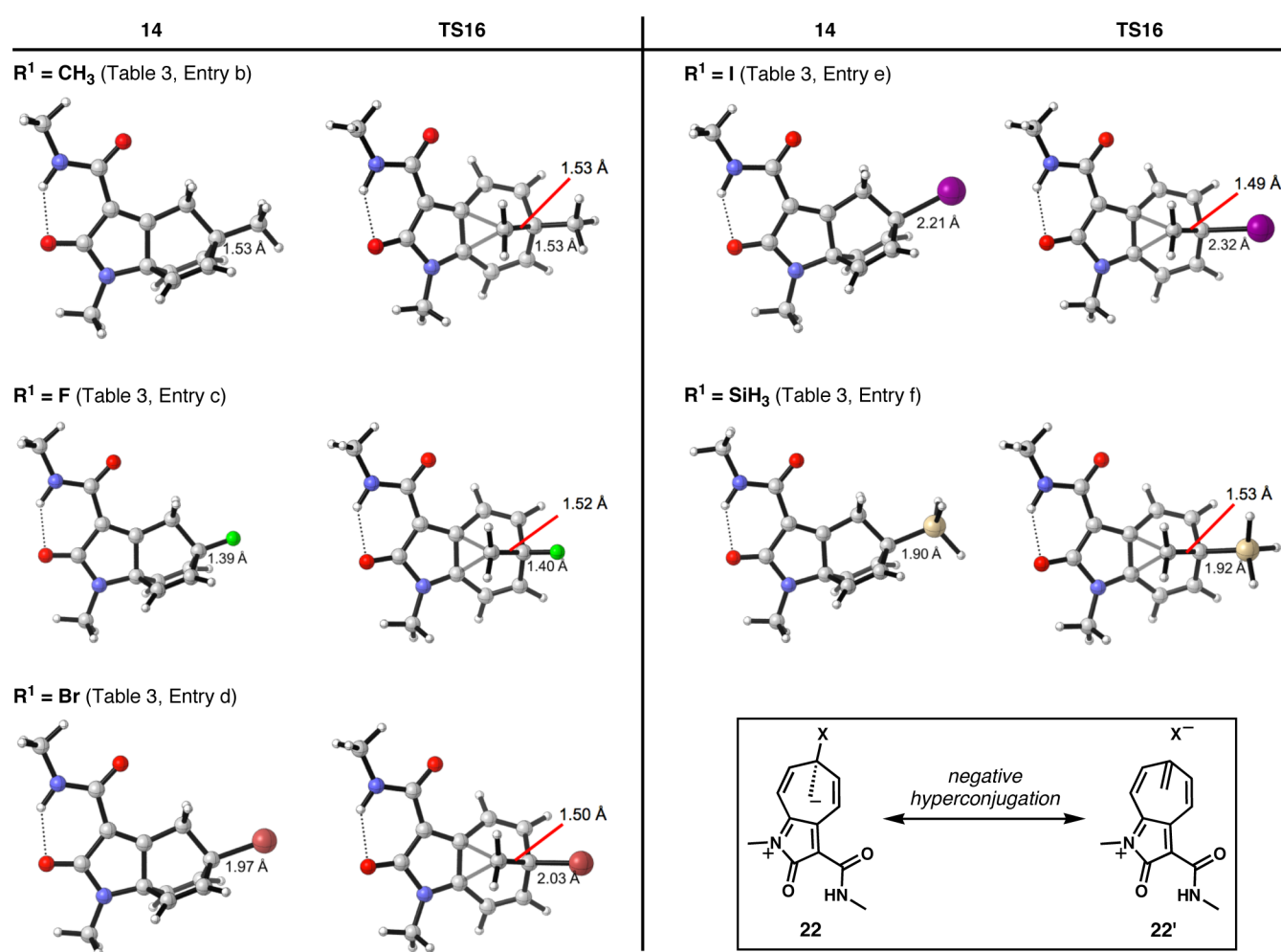


Figure 7. Optimized structures of bridgehead-substituted substrates. The effects of negative hyperconjugation can be seen in the varying bond lengths.

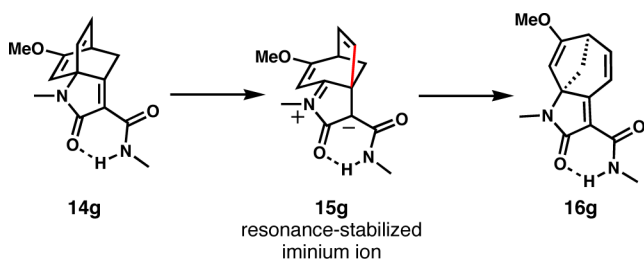
into the σ^* -orbital of the C–X bond allows delocalization of the negative charge buildup. Optimizations in implicit water

support this notion, demonstrating larger bond-length changes in polar solvent. In other words, better leaving groups at the R¹

position result in the bridgehead carbon developing more sp^2 character, stabilizing the excess negative charge.

Substitution on either alkene of the bicyclo[2.2.2]octadiene not only stereoelectronically affects the alkenyl migration but also desymmetrizes the bicycle. Either alkene can participate in the initial migration, which leads to two different products, **16** and **18**. With the electron-donating methoxy group at the R^2 position (entry g), the zwitterionic intermediate **15g** arising from migration of the unsubstituted alkene is more stable than **17g**, owing to the available resonance stabilization of the iminium ion of **15g** through a push–pull system with the lone pair on oxygen (see Scheme 2). Despite the favorability of **15g**,

Scheme 2. Resonance-Stabilization in Intermediate **15g**



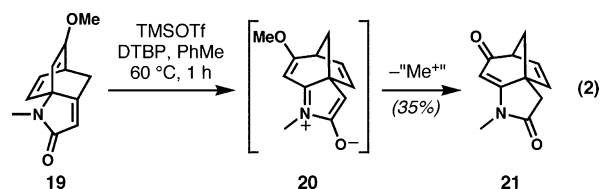
TS18g is 1.4 kcal/mol lower than **TS16g**, in qualitative agreement with the 7:3 ratio of **18g**:**16g** observed experimentally by Himbert.⁵ The methoxy substituent, regardless of whether the migrating alkene was substituted or unsubstituted, has a similar influence on the methylene shift: both **TS16** and **TS18** are favorable relative to the parent amide.

When the methoxy substituent is moved to the R^3 position (entry h), migration of the substituted vinyl group results in a product that is endergonic by 6.0 kcal/mol, which could revert back to starting material. Steric strain arises from the close proximity of the amide and methoxy groups, preventing **18h** from being favored thermodynamically. On the other hand, migration of the unsubstituted vinyl group and subsequent formation of **16h** require overcoming a substantial 38.4 kcal/mol barrier, stemming from the general destabilization by the OMe group also present in the intermediate. This is

corroborated by the sluggish but exclusive formation of **16h** observed by Himbert.⁵

Replacement of the electron-rich methoxy group with the electron-deficient nitro group at both the R^2 and R^3 causes an increase in activation barrier for all possible dyotropic shifts. For the R^2 position (entry i), this increase is attributed to the loss of resonance stabilization; the electron-withdrawing NO_2 offers no assistance to the electron-deficient iminium ion and is actually detrimental to the reaction. Placing the nitro group at the R^3 position (entry j) causes similar steric strain as seen with the methoxy group in entry h. The higher activation barriers for rearrangement coincide with the observation of decomposition of these nitro-substituted compounds in refluxing xylene.⁵

An interrupted dyotropic rearrangement supports the proposed mechanism. We again looked to experiment for validation of the computational results. Our attempt to experimentally generate the dyotropic shift product from methoxy-substituted cycloadduct **19** (lacking the methyl carboxamide activating group) under Lewis acidic conditions did not afford the expected product at all (eq 2); rather, we isolated product **21** in 35% yield. We reasoned that, after the initial vinyl shift to form zwitterion intermediate **20**, demethylation and isomerization generate the “trapped intermediate” **21**, which is then unable to undergo the second 1,2-shift. This observation provides further strong circumstantial evidence for the stepwise shifts involved in these formal dyotropic rearrangements.



Dyotropic Rearrangement of Lactone and Ketone Substrates. Curiously, only dyotropic rearrangements of cycloadducts with nitrogen-containing heterocycles have been reported, despite the large amount of successful Diels–Alder reactions of substrates with other heteroatoms by Himbert.^{3c,g} We also computed the rearrangement pathways of unsaturated lactone, unsaturated thiolactone, and cyclopentenone Himbert

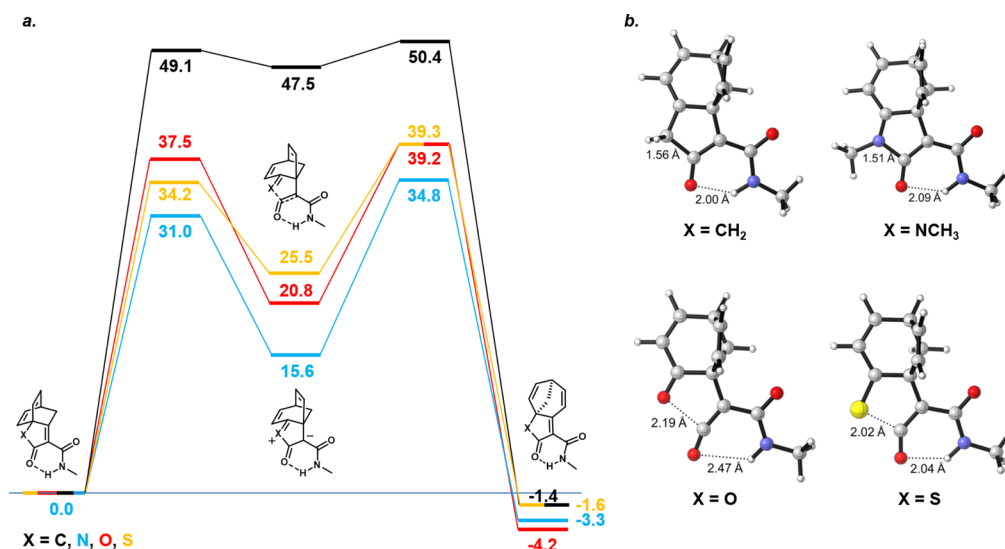


Figure 8. (a) Reaction coordinate diagrams for the formal dyotropic shift of heterologues. (b) Optimized structures of intermediates.

cycloadducts (Figure 8). The overall topology of the reaction coordinate diagram is retained across the different substrates; after the initial vinyl migration, formation of the intermediate is followed by the rate-determining methylene shift, resulting in an exergonic reaction. As expected, the carbon analogue offers no stabilization of the intermediate and transition states. Although the oxygen and sulfur atoms significantly lower the activation barriers relative to the all-carbon case, they are not as effective as the nitrogen atom in the lactam substrate. Interestingly, the intermediates of the sulfur and oxygen analogues were not zwitterionic; rather, the weak $C_{sp^2}-X$ σ -bond breaks to quench the positive charge on the heteroatom, forming a ring-opened ketene intermediate. An intrinsic reaction coordinate calculation and a thorough bond scan each reveals no intermediate between alkenyl migration and ketene formation, suggesting simultaneous occurrence. This unexpected ketene intermediate might be a possible decomposition pathway, which could explain the lack of successful dyotropic shifts reported for these substrates.

CONCLUSIONS

We have investigated the formal dyotropic rearrangements of substituted bicyclo[2.2.2]octadiene moieties to corresponding bicyclo[3.2.1]octadienes discovered by Himbert. The rearrangements are characterized by a stepwise mechanism that proceeds through a zwitterionic intermediate. Substituents that stabilize the partial charges in the rate-determining methylene shift effectively lower the activation barrier, resulting in more facile transformations. Moreover, substitution at the bridgehead carbon of the bicyclo[2.2.2]octadiene leads to an increase in reaction rate owing to negative hyperconjugative effects. Importantly, many aspects of the computational results have been experimentally validated.

Furthermore, computations suggest that the exclusivity of nitrogen-containing compounds participating in the dyotropic rearrangement may be due to the presence of a cumulenic intermediate when replacing nitrogen with oxygen or sulfur, which could lead to decomposition pathways or formation of multiple side products. However, it is conceivable that the dyotropic rearrangement might still occur if the methylene shift precedes out-of-plane rotation or nucleophilic attack of the cumulene. The synthesis of these heterologous compounds and their rearrangement reactions could prove useful in the preparation of additional complex heterocyclic compounds.

ASSOCIATED CONTENT

Supporting Information

Experimental protocols, characterization data, and NMR spectra for new compounds. Computational data are also provided. The Supporting Information is available free of charge on the ACS Publications website at DOI: 10.1021/jacs.5b03718.

AUTHOR INFORMATION

Corresponding Authors

*houk@chem.ucla.edu

*cdv@uci.edu

Author Contributions

§H.V.P. and A.S.K. contributed equally.

Notes

The authors declare no competing financial interest.

ACKNOWLEDGMENTS

A.S.K. was supported by a UC Irvine GAANN fellowship. Work at UC Irvine was supported by the NSF (Awards CHE-0847061 [CAREER] and CHE-1262040) and by Bristol-Myers Squibb. K.N.H. thanks the National Institute of General Medical Sciences, National Institute of Health GM-36770. This work used the Extreme Science and Engineering Discovery Environment (XSEDE), which is supported by National Science Foundation Grant Number OCI-1053575.

REFERENCES

- (1) Schmidt, Y.; Lam, J. K.; Pham, H. V.; Houk, K. N.; Vanderwal, C. D. *J. Am. Chem. Soc.* **2013**, *135*, 7339–7348.
- (2) Lam, J. K.; Schmidt, Y.; Vanderwal, C. D. *Org. Lett.* **2012**, *14*, 5566–5569.
- (3) Selected, particularly relevant references: (a) Himbert, G.; Henn, L. *Angew. Chem., Int. Ed.* **1982**, *21*, 620. (b) Himbert, G.; Diehl, K.; Maas, G. *J. Chem. Soc., Chem. Commun.* **1984**, 900–901. (c) Himbert, G.; Fink, D. *Tetrahedron Lett.* **1985**, *26*, 4363–4366. (d) Henn, L.; Himbert, G.; Diehl, K.; Kaffory, M. *Chem. Ber.* **1986**, *119*, 1953–1963. (e) Himbert, G.; Diehl, K.; Schlindwein, H.-J. *Chem. Ber.* **1986**, *119*, 3227–3235. (f) Himbert, G.; Fink, D. *Z. Naturforsch. B: Chem. Sci.* **1994**, *49*, 542–550. (g) Himbert, G.; Fink, D. *J. Prakt. Chem.* **1994**, *336*, 654–657. (h) Himbert, G.; Fink, D. *J. Prakt. Chem.* **1996**, *338*, 355–362.
- (4) Lam, J. K.; Pham, H. V.; Houk, K. N.; Vanderwal, C. D. *J. Am. Chem. Soc.* **2013**, *135*, 17585–17594.
- (5) Himbert, G.; Diehl, K. *Liebigs Ann./Recueil* **1997**, 1255–1260.
- (6) (a) Reetz, M. T. *Angew. Chem., Int. Ed. Engl.* **1972**, *11*, 129–130. (b) Reetz, M. T. *Angew. Chem., Int. Ed. Engl.* **1972**, *11*, 130–131.
- (7) For a review, see: Fernández, L.; Cossío, F. P.; Sierra, M. A. *Chem. Rev.* **2009**, *109*, 6687–6711.
- (8) (a) Stocks, M.; Kocieński, P.; Donald, D. K. *Tetrahedron Lett.* **1990**, *31*, 1637–1640. (b) Li, W.; LaCour, T. G.; Fuchs, P. L. *J. Am. Chem. Soc.* **2002**, *124*, 4548–4549. (c) Lin, S.; Danishefsky, S. J. *Angew. Chem., Int. Ed.* **2002**, *41*, 512. (d) Denmark, S. E.; Montgomery, J. I. *Angew. Chem., Int. Ed.* **2005**, *44*, 3732–3736. (e) Denmark, S. E.; Montgomery, J. I.; Kramps, L. A. *J. Am. Chem. Soc.* **2006**, *128*, 11620–11630. (f) de Lemos, E.; Porée, F.-H.; Commerçon, A.; Betzer, J.-F.; Pancrazi, A.; Ardisson, J. *Angew. Chem., Int. Ed.* **2007**, *46*, 1917–1921. (g) Leverett, C. A.; Purohit, V. C.; Johnson, A. G.; Davis, R. L.; Tantillo, D. J.; Romo, D. *J. Am. Chem. Soc.* **2012**, *134*, 13348–13356. (h) Ren, W.; Bian, Y.; Zhang, Z.; Shang, H.; Zhang, P.; Chen, Y.; Yang, Z.; Luo, T.; Tang, Y. *Angew. Chem., Int. Ed.* **2012**, *51*, 6984–6988.
- (9) Reetz, M. T. *Tetrahedron* **1973**, *29*, 2189–2194.
- (10) (a) Grob, C. A.; Winstein, S. *Helv. Chim. Acta* **1952**, *35*, 782–802. (b) Kos, A. J.; Jemmis, E. D.; Schleyer, P. v. R.; Gleiter, R.; Fischbach, U.; Pople, J. A. *J. Am. Chem. Soc.* **1981**, *103*, 4996–5002. (c) Frontera, A.; Suñer, G. A.; Deyà, P. M. *J. Org. Chem.* **1992**, *57*, 6731–6735. (d) Mulzer, J.; Hoyer, K.; Müller-Fahrnow, A. *Angew. Chem., Int. Ed. Engl.* **1997**, *36*, 1476–1478. (e) Zhang, X.; Houk, K. N.; Lin, S.; Danishefsky, S. J. *J. Am. Chem. Soc.* **2003**, *125*, 5111–5114. (f) Zou, J.-W.; Yu, C.-H. *J. Phys. Chem. A* **2004**, *108*, S649–S654. (g) Fernández, L.; Sierra, M. A.; Cossío, F. P. *Chem.—Eur. J.* **2006**, *12*, 6323–6330. (h) Yu, Y.; Feng, S. J. *Phys. Chem. A* **2006**, *110*, 12463–12469. (i) Buchanan, J. G.; Ruggiero, G. D.; Williams, I. H. *Org. Biomol. Chem.* **2008**, *6*, 66–72. (j) Davis, R. L.; Tantillo, D. J. *J. Org. Chem.* **2010**, *75*, 1693–1700. (k) Davis, R. L.; Leverett, C. A.; Romo, D.; Tantillo, D. J. *J. Org. Chem.* **2011**, *76*, 7167–7174. (l) Gutierrez, O.; Tantillo, D. J. *J. Org. Chem.* **2012**, *77*, 8845–8850. (m) Fernández, L.; Bickelhaupt, F. M.; Cossío, F. P. *Chem.—Eur. J.* **2012**, *18*, 12395–12403. (n) Braddock, D. C.; Roy, D.; Lenoir, D.; Moore, E.; Rzepa, H. S.; Wu, J. I.-C.; Schleyer, P. v. R. *Chem. Commun.* **2012**, *48*, 8943–8945.
- (11) Himbert, G.; Diehl, K. *Liebigs Ann./Recueil* **1997**, 1255–1260.

(12) (a) Trifonov, L. S.; Orahovats, A. S. *Helv. Chim. Acta* **1986**, *69*, 1585–1587. (b) Trifonov, L. S.; Orahovats, A. S. *Helv. Chim. Acta* **1987**, *70*, 262–270. (c) Trifonov, L. S.; Orahovats, A. S. *Helv. Chim. Acta* **1987**, *70*, 1732–1736. (d) Trifonov, L. S.; Simova, S. D.; Orahovats, A. S. *Tetrahedron Lett.* **1987**, *28*, 3391–3392. (f) Trifonov, L. S.; Orahovats, A. S. *Helv. Chim. Acta* **1989**, *72*, 59–64.

(13) Trifonov, L. S.; Dimitrov, V. S.; Orahovats, A. S. *Helv. Chim. Acta* **1989**, *72*, 502–506.

(14) (a) Becke, A. D. *Phys. Rev. A* **1988**, *38*, 3098–3100. (b) Lee, C.; Yang, W.; Parr, R. G. *Phys. Rev. B* **1988**, *37*, 785–789. (c) Becke, A. D. *J. Chem. Phys.* **1993**, *98*, 5648–5652.

(15) Frisch, M. J.; Trucks, G. W.; Schlegel, H. B.; Scuseria, G. E.; Robb, M. A.; Cheeseman, J. R.; Scalmani, G.; Barone, V.; Mennucci, B.; Petersson, G. A.; Nakatsuji, H.; Caricato, M.; Li, X.; Hratchian, H. P.; Izmaylov, A. F.; Bloino, J.; Zheng, G.; Sonnenberg, J. L.; Hada, M.; Ehara, M.; Toyota, K.; Fukuda, R.; Hasegawa, J.; Ishida, M.; Nakajima, T.; Honda, Y.; Kitao, O.; Nakai, H.; Vreven, T.; Montgomery, J. A., Jr.; Peralta, J. E.; Ogliaro, F.; Bearpark, M.; Heyd, J. J.; Brothers, E.; Kudin, K. N.; Staroverov, V. N.; Keith, T.; Kobayashi, R.; Normand, J.; Raghavachari, K.; Rendell, A.; Burant, J. C.; Iyengar, S. S.; Tomasi, J.; Cossi, M.; Rega, N.; Millam, J. M.; Klene, M.; Knox, J. E.; Cross, J. B.; Bakken, V.; Adamo, C.; Jaramillo, J.; Gomperts, R.; Stratmann, R. E.; Yazyev, O.; Austin, A. J.; Cammi, R.; Pomelli, C.; Ochterski, J. W.; Martin, R. L.; Morokuma, K.; Zakrzewski, V. G.; Voth, G. A.; Salvador, P.; Dannenberg, J. J.; Dapprich, S.; Daniels, A. D.; Farkas, O.; Foresman, J. B.; Ortiz, J. V.; Cioslowski, J.; Fox, D. J. *Gaussian 09*, revision C.01; Gaussian, Inc.: Wallingford, CT, 2010.

(16) (a) Ess, D. H.; Houk, K. N. *J. Phys. Chem. A* **2005**, *109*, 9542–9553. (b) Pieniazek, S. N.; Clemente, F. R.; Houk, K. N. *Angew. Chem., Int. Ed.* **2008**, *47*, 7746–7749.

(17) Stephens, P. J.; Devlin, F. J.; Chabalowski, C. F.; Frisch, M. J. *J. Phys. Chem.* **1994**, *98*, 11623–11627.

(18) Śliwa, P.; Handzlik, J. *Chem. Phys. Lett.* **2010**, *493*, 273–278.

(19) Reed, A. E.; Weinhold, F. *J. Chem. Phys.* **1983**, *78*, 4066–4073. (b) Reed, A. E.; Weinstock, R. B.; Weinhold, F. *J. Chem. Phys.* **1985**, *83*, 735–746.

(20) Cossi, M.; Rega, N.; Scalmani, G.; Barone, V. *J. Comput. Chem.* **2003**, *24*, 669–681.

(21) (a) Marx, J. N.; Hahn, Y.-S. P. *J. Org. Chem.* **1988**, *53*, 2866–2868. (b) Genaev, A. M.; Shubin, V. G. *Russ. Chem. Bull., Int. Ed.* **2006**, *55*, 1085–1088.

(22) (a) Bushmelev, V. A.; Genaev, A. M.; Shubin, V. G. *Russ. J. Org. Chem.* **2004**, *40*, 1007–1013. (b) Artamoshkin, V. G.; Bushmelev, V. A.; Genaev, A. M.; Shubin, V. G. *Russ. J. Org. Chem.* **2006**, *42*, 1279–1285.

(23) Saalfrank, R. W.; Hilbig, K.; Schütz, F.; Peters, K.; von Schnering, H. G. *Chem. Ber.* **1988**, *121*, 1291–1297.

(24) Ye, W.; Li, W.; Zhang, J. *Chem. Commun.* **2014**, *50*, 9879–9882.

(25) Schleyer, P. v. R.; Kos, A. J. *Tetrahedron* **1983**, *39*, 1141–1150.